Journal of Aerosol Science 113 (2017) 178–188

Contents lists available at ScienceDirect

Journal of Aerosol Science

journal homepage: www.elsevier.com/locate/jaerosci

Nonequilibrium ionization of welding fume plasmas; Effect of potassium additional agent on the particle formation

V.I. Vishnyakov[a,*], S.A. Kiro[a], M.V. Oprya[a], O.I. Shvets[b], A.A. Ennan[a]

[a] Physical-Chemical Institute for Environmental and Human Protection, National Academy of Sciences of Ukraine, 3 Preobrazhenska st., Odessa 65082, Ukraine

[b] National University "Odessa Maritime Academy", 8 Didrikhson st., Odessa 65029, Ukraine

ARTICLE INFO

Keywords:
Plasma
Nonequilibrium ionization
Welding fumes
Particle formation rate

ABSTRACT

The ionization balance in the welding fume plasma is studied for shielded metal and gas metal arc welding. The presence of condensed particles causes the ionization of gas atoms on the particle surface and leads to ionization balance displacement in the space charge layer around particle. Therefore, the average electron and ion number densities are changed, when charged particles are present in the plasma. It leads to the nucleation process change and, accordingly, influences the fume formation rate. The measured particle formation rates for different potassium additives in the shielding gas are presented. The calculated nuclei number densities for gas metal arc welding with potassium additive, which correlates well with experimental data, are demonstrated.

1. Introduction

The arc welding is accompanied by emission of the high-temperature metal vapors in environmental air. Mixing of vapors with air leads to their cooling, liquid droplets condensation, droplets solidification and formation of primary particles, their coagulation and formation of inhalable particles in the breathing zone. Inhalable particles have the complex chemical composition, frequently unhealthy. Therefore, welding fumes represent toxicological and ecological danger, to reduce them is necessary to know how to control the chemical and disperse composition of inhalable particles in the process of their formation.

Formation of particles in the welding fumes results from condensation of vapors effusing from the arc zone. Thus, there is heterogeneous ion-induced nucleation, i.e. condensation centers are ions. The ions appear via the vapor atoms ionization, which occurs because of collision with electrons (thermal ionization) and by the interaction with arc UV-radiation. Besides these, the ionization by collisions of atoms with condensed particles also can exists. Thus, there are at least three channels of ionization, which are necessary for considering while describing the ionization balance in the welding fume plasma. It should be taken into account that different ionization-recombination channels influence each other, because each of them changes the number of electrons and ions in the system that leads to change in every channel recombination intensity.

For the first time, probably, Sugden and Thrush (1951) detected the ionization balance displacement in the plasma, containing the condensed particles, while studying the hydrocarbon flames. Similar results have been obtained by Shuler and Weber (1954). They have assumed that the source of excess electrons is the thermionic emission from the particles' surface. The description of plasma ionization, based on the equilibrium of submicron particles with gas phase, was proposed by Einbinder (1957) and was delivered by Smith (1958). Arshinov and Musin (1958a, 1958b) modified Einbinder method for the case of negatively charged particles presence

* Corresponding author.
E-mail addresses: dr.v.vishnyakov@gmail.com, eksvar@ukr.net (V.I. Vishnyakov).

http://dx.doi.org/10.1016/j.jaerosci.2017.08.004
Received 5 July 2017; Received in revised form 25 July 2017; Accepted 11 August 2017
Available online 15 August 2017
0021-8502/

in the plasma. They have obtained the equilibrium constant, as a function of particle size and charge distribution. Gibson (1966) has considered in details the influence of thermionic emission from particle surface on the ionization balance. Further, including up-to-date studies, are basically devoted to determination of electron number density and particle charges (Fortov & Iakubov, 1984; Fortov, Khrapak, Khrapak, Molotkov, & Petrov, 2004; Goree, 1994; Semenov & Sokolik, 1970; Shukla & Mamun, 2002; Sicha, 1979; Sodha & Kaw, 1968; Sodha & Mishra, 2011; Sodha, Palumbo, & Daley, 1963; Zhukhovitskii, Khrapak, & Yakubov, 1984). Ionization balance in the dusty plasma is studied insufficiently.

The presented paper is devoted to ionization balance in the welding fume plasma theoretical studying and also includes experimental researches of plasma ionization on the particle formation effect when gas metal arc welding is used.

2. Charge carriers number densities

Ionization balance in the thermal plasma is described by Saha equation (Kittel, 1969; Landau & Lifshitz, 1976):

$$\frac{n_e n_i}{n_a} = \frac{\Sigma_i}{\Sigma_a}\nu_e \exp\frac{-I}{k_B T} \equiv K_S, \tag{1}$$

where n_e, n_i and n_a are the average for local thermodynamic equilibrium (LTE) region number densities of electrons, ions and atoms, respectively; $n_a = n_A - n_i$, n_A is the initial atom number density; Σ_i and Σ_a are the ion and atom statistical weights;

$$\nu_e = 2\left(\frac{m_e k_B T}{2\pi\hbar^2}\right)^{3/2}$$

is the effective density of the electron states; I is the potential of atom ionization; k_B is the Boltzmann constant; T is the temperature in kelvin; m_e is the electron mass; $\hbar$ is the Plank constant; K_S is the Saha constant.

The arc UV-radiation with photon energy $h\nu \geq I$ effects on the ionization balance. At the shielded metal arc welding (SMAW) the additional agents of potassium with ionization potential $I^K = 4.34$ eV and sodium with ionization potential $I^{Na} = 5.14$ eV are inserted into the plasma from electrode cover, and they determine the plasma ionization degree. The photon flux of UV-radiation from welding arc with photon energy $h\nu \geq 5$ eV is $j_{ph} \sim 10^{15}\mathrm{cm}^{-2}\mathrm{s}^{-1}$. Such radiation intensity influences weakly on ionization balance in the condensation zone at the temperature $T \sim 1800 - 3000$ K. However, in the coagulation zone, when the temperature $T < 1500$ K, ionization by UV-radiation becomes basic. Evolutions of potassium and sodium ionization in the cooling vapor are presented in Fig. 1.

Therefore, Saha constant in equation (1) should be replaced by formula, which considers the UV-radiation (Vishnyakov, Kiro, & Ennan, 2013):

$$K_S = \frac{\Sigma_i}{\Sigma_a}\nu_e \exp\frac{-I}{k_B T} + \frac{\pi r_a^2 j_{ph}}{\gamma_{ei}},$$

where r_a is the ionizable atom radius ($r_a = 0.28$ nm for potassium and $r_a = 0.22$ nm for sodium); γ_{ei} is the electron-ion recombination coefficient $\gamma_{ei} \sim 10^{-6}\mathrm{cm}^3\mathrm{s}^{-1}$ (Pal', Starostin, & Filippov, 2001).

The plasma electrical neutrality means that

$$n_e = n_i = n_0, \tag{2}$$

where n_0 is the unperturbed number density, which is determined from (1):

$$n_0 = \frac{K_S}{2}\left(\sqrt{1 + 4\frac{n_A}{K_S}} - 1\right). \tag{3}$$

The welding fume plasma in the condensation zone contains the droplets of growing nuclei, which interact with plasma ions and electrons. The cooling of welding fume causes the droplet phase transition into solid particles, which also interact with free ions and

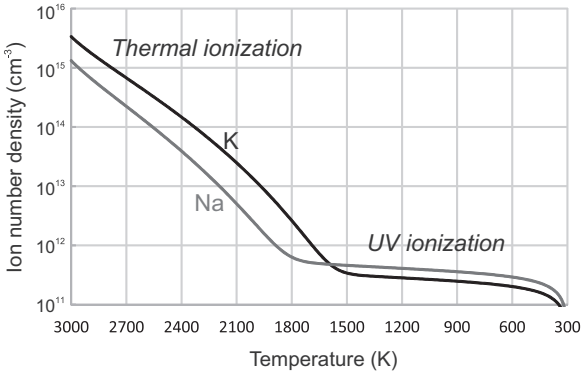

Fig. 1. Typical equilibrium ionization of additional agents in cooling vapor; Content in electrode cover: 3% K and 6% Na.

electrons. The interphase interaction leads to charging of the condensed particles. Thus, the space charge region (SCR) is formed around the charged particles, where displacement of ion and electron number densities in the particle electric field occurs. On the plasma-particle boundary the electron number density determines by the balance between emission electron flux (via thermionic emission and photoemission) (Vishnyakov et al., 2013):

$$I_e^{em} = 4\pi a^2 \frac{4\pi m_e (k_B T)^2}{(2\pi\hbar)^3} \exp\frac{-W}{k_B T} + \pi a^2 Y j_{ph} \tag{4}$$

and backflow of electrons adsorbed by the particle surface at the expense of their sporadic collisions:

$$I_e^{ads} = \pi a^2 v_{eT} n_{es}, \tag{5}$$

where a is the particle radius; W is the electron work function; Y is the quantum yield; $v_{eT} = \sqrt{8k_B T/\pi m_e}$ is the thermal velocity of electrons; $n_{es} = n_0 \exp(V_b/k_B T)$ is the surface electron number density; V_b is the potential barrier on the plasma-particle boundary.

For example, surface electron number density under thermionic emission (without a photoemission) is equal

$$n_{es} = \nu_e \exp\frac{-W}{kT},$$

and, considering the Saha equation (1) for equilibrium ionization in SCR near particle surface: $n_{es} n_{is}/n_{as} = K_S$, it follows for ionization degree near particle surface

$$\frac{n_{is}}{n_{as}} = \frac{\Sigma_i}{\Sigma_a} \exp\frac{W - I}{k_B T}, \tag{6}$$

which is known as Saha - Langmuir equation (Dresser, 1968).

In general case, considering photoemission, surface electron number density

$$n_{es} = \nu_e \exp\frac{-W}{k_B T} + \frac{Y j_{ph}}{v_{eT}}, \tag{7}$$

accordingly, surface ionization degree

$$\frac{n_{is}}{n_{as}} = \frac{\Sigma_i}{\Sigma_a} \exp\frac{W - I}{k_B T} \frac{1}{1 + \frac{Y j_{ph}}{v_{eT} \nu_e} \exp\frac{W}{k_B T}}, \tag{8}$$

and when the temperature $T < 1500$ K,

$$\frac{n_{is}}{n_{as}} \cong K_S \frac{v_{eT}}{Y j_{ph}},$$

i.e. determines by UV-radiation only.

The plasma atoms' ionization degree inside SCR and outside of it (far from the particle) is different. It is caused by additional channels of ionization and recombination on the particle surface that distinguishes SCR from other plasma volume. In papers (Vishnyakov & Dragan, 2005; Vishnyakov, Dragan, & Evtuhov, 2007) it was proposed to consider this fact by introduction of the effective ionization potential depending on the particle electric field. This method is inapplicable for system under consideration because photoionization is taken into account.

There is another approach to this problem (Vishnyakov, 2005, 2006; Vishnyakov & Dragan, 2006). The Boltzmann distribution law usually applies for description of charge carriers in the equilibrium plasma (or in LTE region): $n_e \sim \exp(e\varphi/k_B T)$, $n_i \sim \exp(-e\varphi/k_B T)$. Then SCR can be considered as a region where plasma displacement from equilibrium occurs. Accordingly, the electron and ion number densities can be determined as deviations from equilibrium values:

$$n_e = n_0 \exp\frac{e\varphi}{k_B T} + \delta n, \quad n_i = n_0 \exp\frac{-e\varphi}{k_B T} + \delta n, \tag{9}$$

where deviation δn should be identical for ions and electrons, because the volumetric charge should be preserved.

The nonequilibrium additive was determined as function of the potential (Vishnyakov, 2005):

$$\delta n = n_0 \frac{\exp \Phi - 1}{2\cosh \Phi - 1},$$

from hence follows for electron and ion distributions (Vishnyakov, 2006):

$$n_e = n_0 \frac{\exp(2\Phi)}{2\cosh \Phi - 1}, \tag{10}$$

$$n_i = n_0 \frac{\exp(-2\Phi) + 2\sinh \Phi}{2\cosh \Phi - 1}, \tag{11}$$

where $\Phi = e\varphi/k_B T$ is the dimensionless potential.

The dependencies of nonequilibrium number densities (10) and (11) as ratio to Boltzmann distribution law on the potential are

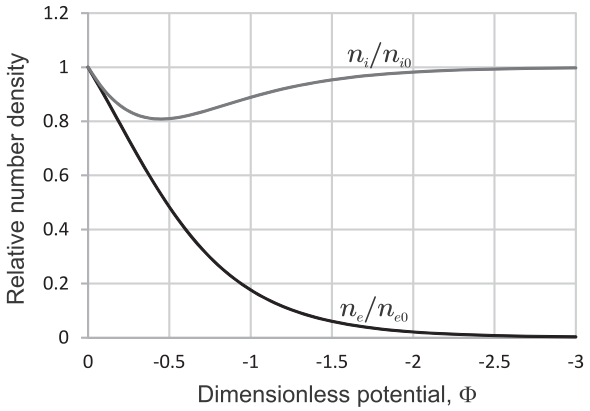

Fig. 2. Dependencies of relative number densities on potential: n_{e0} and n_{i0} are the Boltzmann distributions law.

presented in Fig. 2. The typical for SMAW nucleation zone values were used for calculation: the initial potassium number density $n_A = 10^{17}\text{cm}^{-3}$; the temperature $T = 2700$ K; the work function $W = 4.3$ eV; the photon flux $j_{ph} = 10^{15}\text{cm}^{-2}\text{s}^{-1}$. Only negative potential is considered, because high work function value provides nuclei negative charges (Vishnyakov, Dragan, & Florko, 2008).

The plasma ionization degree decreases in SCR under negative particle charge. However, essential change of the nonequilibrium ion number density occurs only at small values of negative potential. The increase of negative potential leads to strong increasing of the equilibrium ion number. Thus, the nonequilibrium additive becomes negligible in comparison with the Boltzmann distribution law: $n_0 \exp(-\Phi) \gg -\delta n$.

The neutrality condition (2) is still valid in the unperturbed plasma area far from the particles, and the unperturbed number density is determined by Eq. (3). The electron number density is determined by equation (7) near particle surface that allows formulating the equation for potential barrier, using (10):

$$\frac{n_0}{n_{es}} \exp\frac{3V_b}{k_B T} - \exp\frac{2V_b}{k_B T} + \exp\frac{V_b}{k_B T} - 1 = 0, \tag{12}$$

which approximate solution is the expression:

$$V_b \cong \frac{2}{5} k_B T \ln\frac{n_{es}}{n_0}, \quad n_{es} < n_0.$$

The neutrality of the whole plasma volume depends on the charged particles,

$$Z n_p = \overline{n}_e - \overline{n}_i, \tag{13}$$

where Z is the average particle charge in the elementary charges; n_p is the average particle number density; $\overline{n}_e$ and $\overline{n}_i$ are the average on whole volume electron and ion number densities.

The average values of number densities can be calculated via the number of charge carriers, attributable to one particle, i.e. by calculating the integrals from distributions (10) in the Wigner-Seitz cell, which is a sphere with radius $R_W = (3/4\pi n_p)^{1/3}$ around a particle with radius a:

$$N_{eW} = 4\pi \int_a^{R_W} r^2 n_e dr, \quad N_{iW} = 4\pi \int_a^{R_W} r^2 n_i dr. \tag{14}$$

Then, the average on whole volume number densities are equal: $\overline{n}_e = N_{eW} n_p$ and $\overline{n}_i = N_{iW} n_p$. However, for calculations via Eqs. (14) the potential spatial distribution is necessary.

The potential distribution in a particle neighborhood, generally speaking, is unknown, because the solution of the Poisson-Boltzmann equation in spherical symmetry (Vishnyakov et al., 2007) is not known. In the flat case, the solution is function (Vishnyakov & Dragan, 2005)

$$\Phi(r) = 2 \ln\left(\frac{1 + \tanh\frac{\Phi_s}{4} \cdot \exp\frac{a - r}{r_D}}{1 - \tanh\frac{\Phi_s}{4} \cdot \exp\frac{a - r}{r_D}}\right),$$

or in another definition,

$$\tanh\frac{\Phi(r)}{4} = \tanh\frac{\Phi_s}{4} \cdot \exp\frac{a - r}{r_D}, \tag{15}$$

where $\Phi_s = V_b/k_B T$ is the dimensionless potential barrier; $r_D = \sqrt{k_B T/8\pi e^2 n_0}$ is the screening (Debye) length.

The analysis of numerical solution of the Poisson-Boltzmann equation in spherical symmetry allowed to build a function, which

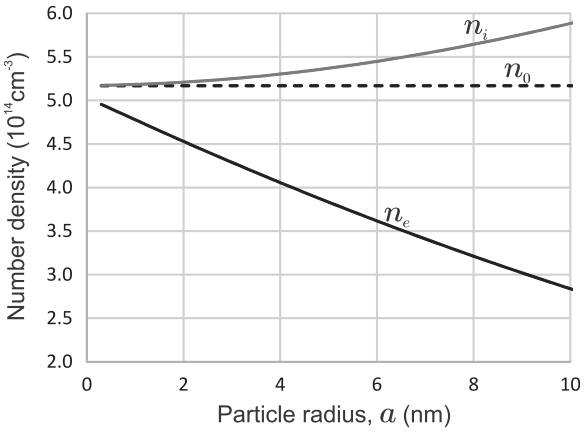

Fig. 3. Dependencies of the average number densities on the particle radius.

correlates effectively with this numerical solution:

$$\tanh\frac{\Phi(r)}{4+\frac{r_D}{a}} = \tanh\frac{\Phi_s}{4+\frac{r_D}{a}}\cdot\frac{a}{r}\exp\frac{a-r}{r_D}, \tag{16}$$

and, if the potential barrier height is subject to condition

$$\exp\left|\frac{\Phi_s}{2}\right| \le 10\frac{r_D}{a}, \tag{17}$$

then function (16) correlates well with the known Debye potential distribution

$$\varphi(r) = \frac{V_b}{e}\frac{a}{r}\exp\frac{a-r}{r_D}.$$

In calculations it is necessary to consider the dependency of the work function on the particle size, which is essential for nanosized particles, such as nuclei (Smirnov, 1997):

$$W(a) = W_0 + \frac{0.39e^2}{a},$$

where W_0 is the work function for flat surface.

The calculating results for average electron and ion number densities as functions of particle radius with taken into account of nonequilibrium ionization are presented in Fig. 3.

The number of charge carriers in the Wigner-Seitz cell determines a particle charge in conformity with neutrality condition (13): $Z = N_{eW} - N_{iW}$. Dependencies of the particle charges on their radius are presented in Fig. 4 for different values of the particle number density. The fractional values of charge are caused by averaging. The charge of 0.1 electron should be understood as 1 electron for 10 particles.

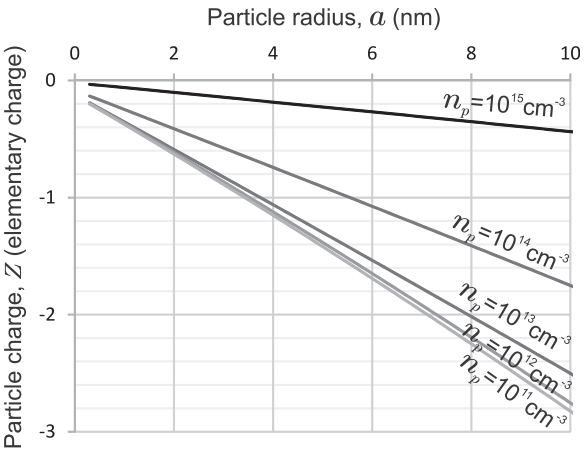

Fig. 4. Dependencies of particle charge on the particle radius.

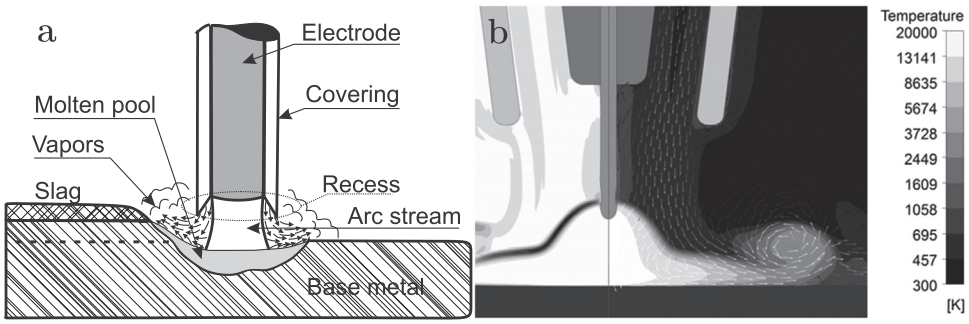

Fig. 5. Schematic drawing of SMAW (a); numerical simulation of GMAW (Dreher, Füssel, & Schnik, 2009) (b).

The average charge carriers' number density has order of 10^{14}cm^{-3} in the plasma under consideration. Therefore, only one free electron falls to ten particles under particle number density $n_p \sim 10^{15}\text{cm}^{-3}$. Such a system can't be described in homogeneous approach and previously used integration on Wigner-Seitz cell (14) is not suitable. In this case such a procedure should apply to charged particles only. The averaging should consider the relation between charge carrier and particle number densities.

Reduction of the particle number density leads to charge growth. The particle charge ceases to depend on particle number density at its low value, because there are enough electrons for charging of the particle to the equilibrium charge.

3. Evolution of the ion number density under welding fume cooling

Ion number density is of special interest for welding fume plasma, because the ions are the condensation centers at the ion-induced nucleation. The additional agent of alkali metals, which is presented in the electrode covering, is the ions' source when SMAW is used. The interior part of electrode burns out more promptly than the exterior cover during welding process. Therefore, recess, in which the vapor ionization occurs, is formed (see Fig. 5a). The alkali additional agent intensively immerses UV-radiation from arc. Therefore, only the long-wave radiation with photon energy $h\nu < 4.3$ eV (potassium ionization potential) penetrates into environment, which corresponds to wave length $\lambda > 288$ nm.

Thus, already ionized vapors effuse into environment. For example, electrodes covered with carbonate-fluorite ($CaCO_3$-CaF_2) Paton UONI 13/55 (American Welding Society classification E6015) contains 3% of potassium and 6% of sodium. The individual Saha constant is calculated for each additional agent metal: K_S^K and K_S^{Na}. The resultant equilibrium unperturbed number density is determined as

$$n_0 = \frac{K_S^K}{2}\left(\sqrt{1 + 4\frac{n_A^K}{K_S^K}} - 1\right) + \frac{K_S^{Na}}{2}\left(\sqrt{1 + 4\frac{n_A^{Na}}{K_S^{Na}}} - 1\right), \tag{18}$$

where initial values of the atom number densities n_A^K and n_A^{Na} are determined by vapor-air mixture formation.

The cooling of the vapor-air mixture is defined by the turbulent mixing of the mass flow of vapors from the arc zone J_{vap} with air (Vishnyakov, Kiro, & Ennan, 2014). The mass flow of entrainment of the air J_{air} can be approximately considered as directly-proportional to flow rate of the vapor-gas mixture $J_{mix} = J_{air} + J_{vap}$, i.e. is described by the following equation:

$$\frac{dJ_{air}}{dt} = \frac{dJ_{mix}}{dt} = \alpha_T J_{mix},$$

where α_T is the factor, which is defined by the initial conditions of the efflux of vapors from the arc zone.

Hence, it follows, that $J_{mix} = J_{vap}\exp(\alpha_T t)$, $J_{air} = J_{val}[\exp(\alpha_T t) - 1]$ and the condensable components' mass fractions in the vapor-air mixture are determined in the following form: $g_i = g_{i0}J_{vap}/J_{mix} = g_{i0}\exp(-\alpha_T t)$, where g_{i0} is the initial component content in vapors.

Accordingly, the air mass fraction in mixture: $g_{air} = 1 - \exp(-\alpha_T t)$, and the effective molecular mass of mixture is $\mu_{mix} = [\sum (g_i/\mu_i) + g_{air}/\mu_{air}]^{-1}$, where μ_i is the components' molecular mass; μ_{air} is air the molecular mass.

Then the current number density of the component atoms can be describes by equation:

$$n_A^i = \frac{P_i}{k_B T} = \frac{g_i \mu_{mix}}{\mu_i}\frac{P}{k_B T}, \tag{19}$$

where P_i is the component partial pressure; P is the atmospheric pressure.

Under assumption that a change in temperature of vapor-air mixture occurs only by mixing with shielding gas, the current temperature can be described as:

$$T(t) = T_\infty + (T_0 - T_\infty)\exp(-\alpha_T t), \tag{20}$$

where T_0 is the initial vapor temperature; T_∞ is the air temperature.

The dependencies of the alkali metal atoms' number densities on the temperature is determined by Eqs. (19) and (20). Resultant

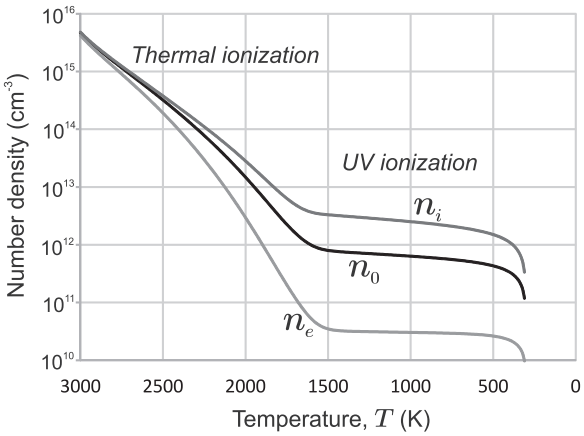

Fig. 6. Evolutions of the electron and ion number densities under vapor-air mixture cooling, when SMAW is used (particle number density is 10^{13}cm^{-3}).

evolutions of the electron and ion number densities under vapor-air mixture cooling are presented in Fig. 6. The unperturbed number density is determined by equilibrium Saha equation. The average electron and ion number densities are calculated by equations (14) with taken into account of the ionization balance displacement in SCR. It is clear that equilibrium displacement is increased under the temperature decrease, when the photoionization starts to play the key role.

The welding fumes obtained under gas metal arc welding (GMAW) do not contain the alkali additional agent. The arc UV-radiation is not absorbed by alkali metal atoms as in case of SMAW, therefore short-wave radiation penetrates into environment that, for example, causes intensive formation of ozone, when GMAW is used. The condensable atoms are the source of ions.

The high-temperature metal vapors from the weld materials mix up with shielding gas under the welding torch nozzle. As it follows from numerical simulation (Dreher et al., 2009), results of which are shown in Fig. 5b, the gas average temperature in the boundary region at the torch outlet $T \sim 2500$ K. It means that nucleation occurs in the vapor-shielding gas mixture, before mixing with air. Therefore, shielding gas instead of air should be used in calculation of the vapor mixing, and, accordingly, the temperature of shielding gas $T_\infty = T_{sg}$ should be used in Eq. (20).

The rate of condensable atoms' thermal ionization is weaker than in alkali metals case, because the ionization potential is higher (for iron $I^{Fe} = 7.9$ eV, for manganese $I^{Mn} = 7.4$ eV). However, the photoionization rate is more intensive because of the increasing photon flux at GMAW: $j_{ph} \sim 10^{16}$cm^{-2}s^{-1}.

The equilibrium number densities of the ions from condensable materials are presented in Fig. 7 for initial mass fractions, which are determined by the welding wire composition: $g_{Fe} = 0.965$ for iron; $g_{Mn} = 0.02$ for manganese; $g_{Si} = 0.01$ for silicon; $g_{Cu} = 0.005$ for copper.

The results of the nonequilibrium ionization calculations are presented in Fig. 8. Effect of the nonequilibrium ionization is higher when GMAW is used in comparison with SMAW. It is caused by more low ionization degree. The Saha - Langmuir equation (6) gives the surface ionization degree for high ionization potential much lower, than for alkali metals. It leads to more appreciable ionization balance displacement at the expense of nonequilibrium additive δn (9).

Addition of the alkali metal into shielding gas should lead to the ion number density increase. Ion number densities evolutions at vapor-gas mixture cooling for the different content of potassium in the shielding gas are presented in Fig. 9. At the initial time

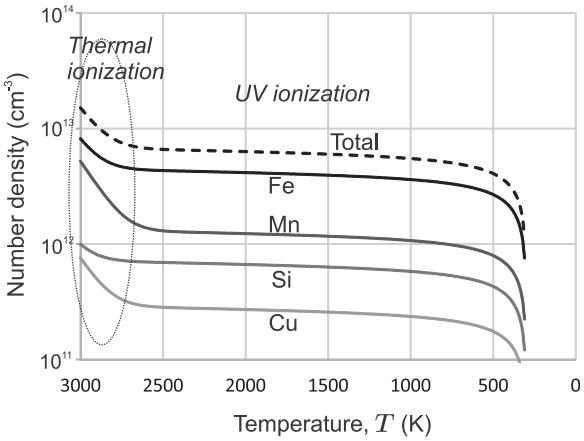

Fig. 7. Evolutions of the equilibrium ion number densities under vapor-gas mixture cooling, when GMAW is used.

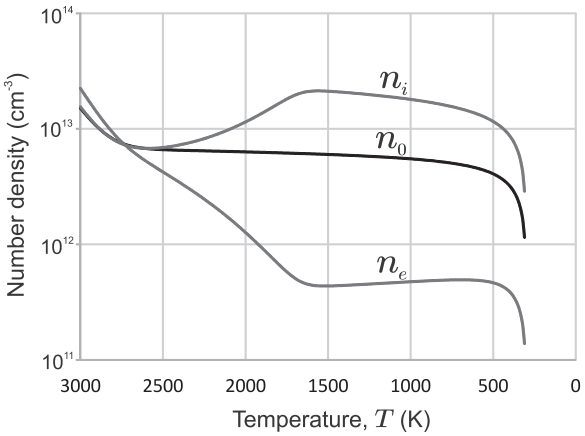

Fig. 8. Evolutions of the electron and ion number densities under vapor-gas mixture cooling with taken into account nonequilibrium ionization, when GMAW is used (particle number density is 10^{13}cm^{-3}).

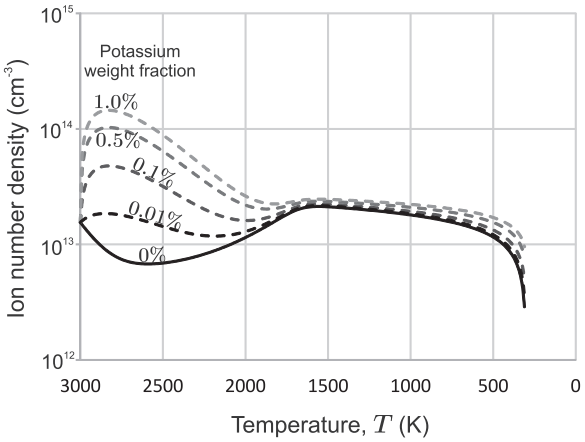

Fig. 9. Evolutions of the ion number densities under vapor-gas mixture cooling, when GMAW with additional potassium is used (particle number density is 10^{13}cm^{-3}).

moment (at temperature of 3000 K) mixing is absent, and the ion number density is determined by the initial vapor composition. However, in process of vapors with shielding gas mixing there is ion number density increasing, which is caused by potassium added in the shielding gas. Even very low content of the potassium additive (0.01%) leads to essential increase of ion number density and, accordingly, electrons, which affects the nucleation and nuclei growth.

4. Experimental study of the effect of potassium additive on particle formation rate

The scheme of experimental equipment, which was used for welding fume particle formation rate measurement, is shown in Fig. 10. Welding fume was generated by the welding on rotated flat mild steel plates with thickness of 10 mm under the stationary torch inside the fume chamber. The DC MMA/TIG/MIG/MAG Paton PSI-250R invertor rectifier was used for producing welding fumes using ER 70S-6 welding wire with 0.8 mm diameter. The reverse polarity (i.e. electrode wire is positive and the plate is negative) direct current of 95 ± 5 A and voltage of 20 ± 0.2 V, and wire feed speed of 8.6 ± 0.1 cm/s were used, as the manufacturer of the electrode wire recommends. A constant contact tube to workpiece distance 9 mm and the angle 90° measured between the plate and the wire axis was maintained throughout all tests.

Potassium injection into shielding gas (CO_2) was carried out using pneumatic medical nebulizer (Vega Technologies Inc.) with outlet stainless-steel grid (100 μm). A flow (4 Lpm) of dry carbon dioxide is used to nebulize the aqueous solution of potassium carbonate. The nebulized aerosol droplets are entered directly into the mixing/drying chamber through the center hole of the stainless-steel porous plate. Teflon rings seal the porous plate along the perimeter and at the center hole. Dry carbon dioxide co-flow (5 Lpm) is introduced into the mixing/drying chamber below the porous plate. The gaseous co-flow is necessary for providing total shielding gas flow, necessary for welding, both drying the droplets and transporting the resulting aerosol into the welding torch gas nozzle (internal diameter 15 mm) with minimum wall losses. Mass flow rate of the nebulized solution was determined by measuring the nebulizer weight changes over the flow period for each test.

The welding fume plume was localized by extracting air at a distance of 20 cm from the welding arc with a flow of 1.7m^3/min and

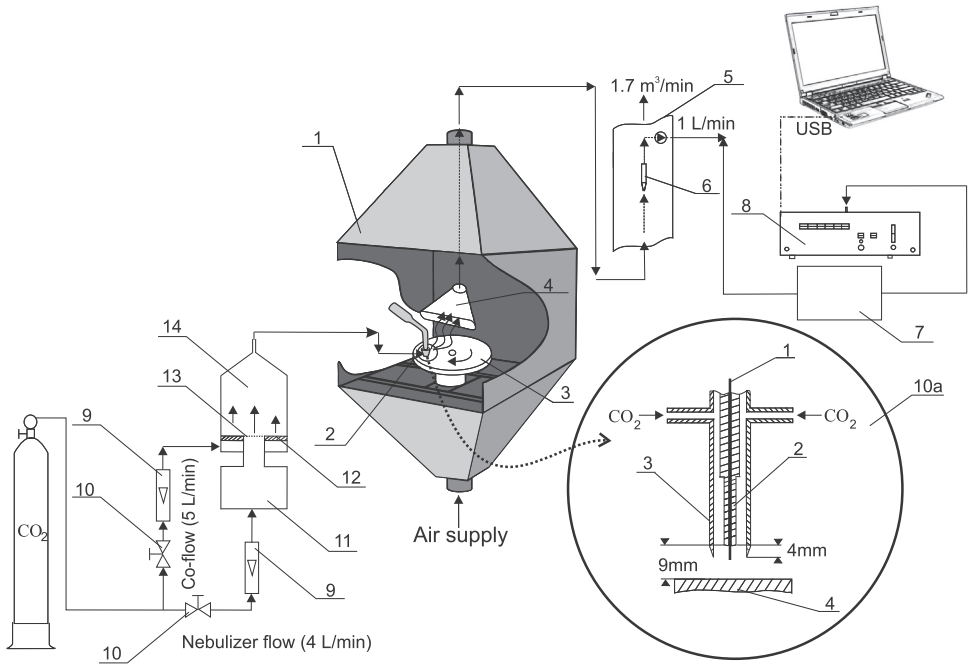

Fig. 10. Experimental equipment scheme: 1, fume chamber; 2, welding torch; 3, turntable; 4, slit air inlet; 5, vertical pipe; 6, nozzle for isokinetic sampling; 7, dual-stage aerosol dilution system; 8, laser aerosol spectrometer; 9, air flow meters; 10, gas cocks; 11, nebulizer; 12, stainless-steel porous plate; 13, stainless-steel grid; 14, mixing/drying chamber. Torch scheme: 1, electrode wire; 2, contact tube; 3, welding torch nozzle (internal diameter 15 mm); 4, mild steel plate.

redirected into the vertical pipe for isokinetic sampling of welding fume with flow rate of 1 Lpm. The total particle number in the sample of welding fume was measured using the laser aerosol spectrometer (LAS-P, 2010). The maximum relative error in determining the particle sizes and their number density is 5% and 10%, respectively, when the particle number density in a sample flow is less than $2 \times 10^3 \mathrm{cm}^{-3}$. The particle number density in the sample has the typical value of $10^5\ \mathrm{cm}^{-3}$. Therefore, the dual-stage aerosol dilution system with the total dilution ratio of 230 for sample flow rate 1 Lpm was used. Petryanov's filters with the collection efficiency of at least 99.99% for the particles with size of 0.15–0.2 μm were used in the dilution system.

The measured by LAS-P number of particles in sample was recalculated in particle formation rate while taking into account the extracting fume flow rate and dilution ratio. The results are presented in Fig. 11 for different potassium weight fraction in the shielding gas. This dependency demonstrates decreasing of the particle generation rate with potassium fraction increasing.

5. Nucleation modelling and discussion

The welding fume formation is the result of heterogeneous ion-induced nucleation in the environment enriched by the electrons. Thus, there is an exchange of energy and charges between the nucleus and the environment. Such consideration has been proposed by

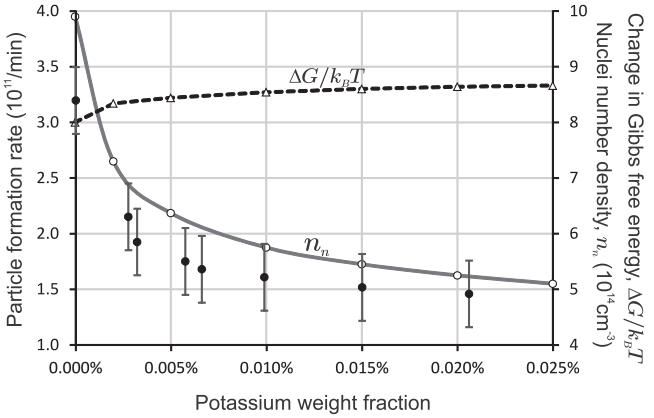

Fig. 11. Effects of potassium weight fraction in CO_2 on the measured particle formation rate (black dots), nuclei number density and change in Gibbs free energy of nucleus formation.

Vishnyakov, Kiro, and Ennan (2011, 2013), where the change in Gibbs free energy as a result of nucleation is determined in the following form:

$$\Delta G = 4\pi r_n^2 \gamma - \frac{4}{3}\pi r_n^3 \frac{\rho k_B T \ln(S)}{m_{ca}} + E_\gamma + E_{ex} + E_q, \tag{21}$$

where r_n is the nucleus radius; $\gamma = \gamma_0 r_n/(r_n + 2\delta)$ is the surface free energy of the nucleus; γ_0 is the surface free energy of the flat; δ is the Tolmen length; m_{ca} is the mass of the condensable atoms; ρ is the nucleus density; S is the supersaturation of the condensable material.

In Eq. (21), the first two terms describes the change in Gibbs free energy defined by the classical nucleation theory. The term E_γ is the change in surface free energy as a result of the double layer on the nucleus surface formation, which can be considered by Lippmann equation (Yeo & Chang, 2005):

$$\frac{d\gamma}{dV_b} = -\frac{Z_n}{4\pi r_n^2},$$

where Z_n is the nucleus charge number, and hence, in Coulomb approximation,

$$E_\gamma = -\frac{Z_n V_b}{2};$$

E_{ex} is the change in Gibbs free energy as a result of the interphase energy exchange:

$$E_{ex} = -Z_n \left(W_n + \frac{3}{2}k_B T\right);$$

E_q is the change in Gibbs free energy as a result of change in the electrostatic energy, which in classical theory (Reist, 1984) is described as

$$E = \frac{e^2}{2}\left(\frac{1}{\varepsilon} - 1\right)\left(\frac{1}{r_i} - \frac{1}{r_n}\right),$$

where ε is the dielectric constant; r_i is the radius of the single-charged positive ion, which induced the nucleation. With taking into account the possible nucleus charge, it has a different definition for the conductor and dielectric:

$$E_{qm} = \frac{e^2}{2}\left[\frac{Z_n^2}{r_n} + \frac{1}{r_n} - \frac{1}{r_i}\right] - \text{for conductor},$$

$$E_{qd} = \frac{e^2(\varepsilon - 1)}{2\varepsilon}\left[\frac{6}{5}\frac{Z_n^2}{(\varepsilon - 1)r_n} + \frac{1}{r_n} - \frac{1}{r_i}\right] - \text{for dielectric}.$$

The number density of equilibrium nuclei with radius $r_n = r_{eq}$ is determined in the following form (Vishnyakov et al., 2013):

$$n_n = \frac{n_{a0}}{N_{an} + N_{an}^{-3/2} \exp\frac{\Delta G(r_{eq})}{k_B T}}, \tag{22}$$

where n_{a0} is the initial (prior to the nucleation start) condensable atom number density; N_{an} is the number of atoms in one nucleus.

The dependency of the nuclei number density on the potassium weight fraction in the shielding gas is demonstrated in Fig. 11. This number density is decreased with potassium fraction increase. The cause of the nuclei number density decrease lies in interphase interaction, which leads to the negative nuclei charge growth. Addition of the potassium into shielding gas causes the change in the nuclei charge Z_n and potential barrier height V_b, because the additional electrons appear in the plasma. Accordingly, it leads to the growth of terms E_{ex}, E_q and E_γ (E_γ can be neglected) in Eq. (21). Therefore, the change in Gibbs free energy is increased with the increase of potassium additive. It is demonstrated in Fig. 11. As it follows from Eq. (22), the increase of $\Delta G(r_{eq})$ cased the nuclei number density decrease.

The nuclei number density determines all other processes, such as nuclei growth and coalescence, and primary particles' formation. Therefore, this density determines the generation rate of the welding fume. Thus, decreasing of the nuclei number density should be correlated with measured particle formation rate, which is demonstrated in Fig. 11.

6. Conclusion

The surface of charged condensed particle is the source of nonequilibrium plasma ionization, which determines the average electron and ion number densities. It is the self-consistent process, because electron and ion number densities determine the particle charge and, accordingly, influences both homogeneous (Vishnyakov, 2008) and heterogeneous (Vishnyakov et al., 2011) nucleation.

Potassium additives to the shielding gas leads to change in nuclei number density, when gas metal arc welding is used. The potassium additives causes the electron and ion number densities increase, which leads to the negative nuclei charge increase and to the growth of change in Gibbs free energy when nucleation occurs. It causes the nuclei number density decrease while the potassium additive increases.

The nuclei number density determines the rate of welding fume particle formation. Therefore, addition in the shielding gas of

potassium should lead to reduction of the fume formation rate that reduces environment pollution and toxicological hazard. Besides, the presence of alkali metal atoms in vapors reduces the ozone emission.

This theoretical conclusion well meets the experimental data, which demonstrates the reduction of the particle formation rate when the potassium fraction in the shielding gas is increased.

References

Arshinov, A. A., & Musin, A. K. (1958a). Thermionic emission from carbon particles. *Soviet Physics Doklady*, *3*, 99–101.

Arshinov, A. A., & Musin, A. K. (1958b). Equilibrium ionization of particles. *Soviet Physics Doklady*, *3*, 588–592.

Dreher, M., Füssel, U., & Schnik, M. (2009). *Simulation of shielding gas flowinside the torch and in the process region of GMA welding. Mathematical modelling of weld phenomena. vol. 9*, Technical University of Dresden127–138.

Dresser, M. J. (1968). The Saha-Langmuir equation and its application. *Journal of Applied Physics*, *39*, 338–339.

Einbinder, H. (1957). Generalized equation for the ionization of solid particles. *Journal of Chemistry Physics*, *26*, 948–956.

Fortov, V. E., & Iakubov, I. T. (1984). *The physics of non-ideal plasma*. Chernogolovka: OIKhF (Translated into English 2000, Singapore: World Scientific).

Fortov, V. E., Khrapak, A. G., Khrapak, S. A., Molotkov, V. I., & Petrov, O. F. (2004). Dusty plasmas. *Physics-Uspekhi*, *47*, 447–492.

Gibson, E. G. (1966). Ionization phenomena in a gas-particles plasma. *The Physics of Fluids*, *9*, 2389–2399.

Goree, J. (1994). Charging of particles in plasma. *Plasma Sources Science and Technology*, *3*, 400–406.

Kittel, C. (1969). *Thermal physics*. New York: Wiley.

Landau, L. D., & Lifshitz, E. M. (1976). *Statisticheskaya Fizika (Statistical Physics), vol. 1*. Moscow: Nauka (Translated into English 1980, Oxford: Pergamon).

LAS-P (2010). *Laser Aerosol Spectrometer (LAS-P) model 9814.290.000*. Moscow: Karpov Institute of Physical Chemistry.

Pal', A. F., Starostin, A. N., & Filippov, A. V. (2001). Charging of dust grains in a nuclear-induced plasma at high pressures. *Plasma Physics Reports*, *27*(2), 143–152.

Reist, P. C. (1984). *Introduction to aerosol science*. New York: Macmillan Publishing.

Semenov, E. S., & Sokolik, A. S. (1970). Thermal and chemical ionization in flames combustion. *Explosion Shock Waves*, *6*(1), 33–43.

Shukla, P. K., & Mamun, A. A. (2002). *Introduction to dusty plasma physics*. Bristol: Institute of Physics.

Shuler, K. E., & Weber, J. (1954). A microwave investigation of the ionization of hydrogen-oxygen and acetylene-oxygen flames. *Journal of Chemistry Physics*, *22*, 491–502.

Sicha, M. (1979). Measurement of the electron energy distribution function in a flame plasma at atmospheric pressure. *Czechoslovak Journal of Physics*, *29*, 640–645.

Smirnov, B. M. (1997). Processes in plasma and gases involving clusters. *Physics-Uspekhi*, *40*, 1117–1147.

Smith, F. T. (1958). On the ionization of solid particles. *Journal of Chemistry Physics*, *28*, 746–747.

Sodha, M. S., & Kaw, P. K. (1968). Field emission from negatively charged solid particles. *Journal of Physics D: Applied Physics*, *1*, 1303–1307.

Sodha, M. S., & Mishra, S. K. (2011). Validity of Saha's equation of thermal ionization for negatively charged spherical particles in complex plasmas in thermal equilibrium. *Physics of Plasmas*, *18*(1–4), 044502.

Sodha, M. S., Palumbo, C. J., & Daley, J. T. (1963). Effect of solid particles on electromagnetic properties of rocket exhausts. *British Journal of Applied Physics*, *14*, 916–919.

Sugden, T. M., & Thrush, B. A. (1951). A cavity resonator method for electron concentration in flames. *Nature*, *168*, 703–704.

Vishnyakov, V. I. (2005). Interaction of dust grains in strong collision plasmas: Diffusion pressure of nonequilibrium charge carriers. *Physics of Plasmas*, *12*(1–6), 103502.

Vishnyakov, V. I. (2006). Electron and ion number densities in the space charge layer in thermal plasmas. *Physics of Plasmas*, *13*(*1–4*), 033507.

Vishnyakov, V. I. (2008). Homogeneous nucleation in thermal dust-electron plasmas. *Physical Review E*, *78*(1–5), 056406.

Vishnyakov, V. I., & Dragan, G. S. (2005). Electrostatic interaction of charged planes in the thermal collision plasma: Detailed investigation and comparison with experiment. *Physical Review E*, *71*(1–9), 016411.

Vishnyakov, V. I., & Dragan, G. S. (2006). Ordered spatial structures of dust grains in the thermal plasma. *Physical Review E*, *73*(1–7), 026403.

Vishnyakov, V. I., Dragan, G. S., & Evtuhov, V. M. (2007). Nonlinear Poisson-Boltzmann equation in spherical symmetry. *Physical Review E*, *76*(1–5), 036402.

Vishnyakov, V. I., Dragan, G. S., & Florko, A. V. (2008). The formation of negatively charged particles in thermoemission plasmas. *Journal of Experimental and Theoretical Physics*, *106*, 182–186.

Vishnyakov, V. I., Kiro, S. A., & Ennan, A. A. (2011). Heterogeneous ion-induced nucleation in thermal dusty plasmas. *Journal of Physics D: Applied Physics*, *44*(*1–7*), 215201.

Vishnyakov, V. I., Kiro, S. A., & Ennan, A. A. (2013). Formation of primary particles in welding fume. *Journal of Aerosol Science*, *58*, 9–16.

Vishnyakov, V. I., Kiro, S. A., & Ennan, A. A. (2014). Multicomponent condensation in the plasma of welding fumes. *Journal of Aerosol Science*, *74*, 1–10.

Yeo, L. M., & Chang, H.-C. (2005). Static and spontaneous electrowetting. *Modern Physics Letters B*, *19*(12), 549–569.

Zhukhovitskii, D. I., Khrapak, A. G., & Yakubov, I. T. (1984). Ionization equilibrium in a highly nonideal plasma containing a condensed dispersed phase. *High Temperature*, *22*, 643–650.